A Very Compact, High Speed and Rugged Acousto-Optic Tunable Filter for Wavelength Division Demultiplexing in Fiber Optic Communication Networks

(SBIR PHASE I CONTRACT)

FINAL REPORT

Sponsored by

U.S. NAVY

Managed Under

Contract #N 62269-94-C-1140

TECHNICAL MONITOR:	Dr. Warren Rosen
NAME OF CONTRACTOR:	Brimrose Corporation of America
PRINCIPAL INVESTIGATOR:	Dr. Sean X. Wang
INVESTIGATORS:	Dr. Vladimir Pelekhaty Mr. Keith Li Mr. Jack Crystal
EFFECTIVE DATE OF CONTRACT:	July 27, 1994
CONTRACT EXPIRATION DATE:	June 30, 1995

brimrose
5020 campbell blvd., baltimore, md 21236 ● tel: 410/931-7200 ● fax: 410/931-7206

REPORT DOCUMENTATION PAGE

Form Approved
OMB No. 0704-0188

1. AGENCY USE ONLY (Leave blank)	2. REPORT DATE	3. REPORT TYPE AND DATES COVERED
	950911	949727 - 950831 (Final)

4. TITLE AND SUBTITLE A Very Compact, High Speed and Rugged Acousto-Optic Tunable Filter for Wavelength Division Demultiplexing in Fiber Optic Communication Networks

5. FUNDING NUMBERS
N62269-94-C1140
P.R. #N00019-94-RXB762R

6. AUTHOR(S)
Dr. Sean X. Wang, PI
Dr. Vladimir Pelekhaty, Mr. Keith Li,
Mr. Jack Crystal

7. PERFORMING ORGANIZATION NAME(S) AND ADDRESS(ES)
Brimrose Corporation of America
5020 Campbell Blvd., Suite E
Baltimore, Maryland 21236

8. PERFORMING ORGANIZATION REPORT NUMBER

9. SPONSORING/MONITORING AGENCY NAME(S) AND ADDRESS(ES)
U.S. Navy, Naval Air Warfare Center,
Aircraft Division
Warminster, PA

10. SPONSORING/MONITORING AGENCY REPORT NUMBER

11. SUPPLEMENTARY NOTES

12a. DISTRIBUTION/AVAILABILITY STATEMENT
Approved for public release; distribution is unlimited

12b. DISTRIBUTION CODE

13. ABSTRACT *(Maximum 200 words)*

Novel concepts of near-collinear/collinear acousto-optic interactions have been investigated during this SBIR Phase I program. As a result, several new acousto-optic tunable filters have been built and tested. The program is highlighted by:

1) Design, fabrication and experimental demonstration of a novel TeO_2 near-collinear acousto-optic tunable filter has been designed, fabricated and tested. *The device exhibits a 1.29 nm spectral resolution and a 160 mw RF drive power at 1523 nm.*; 2) Design, fabrication and experimental demonstration of a novel polarization insensitive TeO_2 near-collinear acousto-optic tunable filter. For random input light, *an overall insertion loss < 3 dB has been achieved.*; 3) Design, fabrication and experimental demonstration of a novel collinear acousto-optic tunable filter. The filter exhibits a *spectral resolution of 1.12 nm @ 1523nm with a low insertion loss.*; 4) The commercial spin-off also has been accomplished at the end of the program. A commercially available fiber pigtailed near-collinear AOTF is shown in the photo. Commercial sales have been generated and new AOTFs have been delivered to customers for applications in optical fiber communications and sensors.

14. SUBJECT TERMS
Acousto Optics, Tunable Filter, Fiber Communications, Wavelength-Division-Multiplexing

15. NUMBER OF PAGES
20

16. PRICE CODE

17. SECURITY CLASSIFICATION OF REPORT	18. SECURITY CLASSIFICATION OF THIS PAGE	19. SECURITY CLASSIFICATION OF ABSTRACT	20. LIMITATION OF ABSTRACT
UC	UC	UC	SAR

NSN 7540-01-280-5500

Standard Form 298 (Rev. 2-89)
Prescribed by ANSI Std. Z39-18
298-102

A Very Compact, High Speed and Rugged Acousto-Optic Tunable Filter for Wavelength Division Demultiplexing in Fiber Optic Communication Networks

PHASE I CONTRACT

FINAL REPORT - TABLE OF CONTENTS

I. EXECUTIVE SUMMARY

Novel concepts of near-collinear/collinear acousto-optic interactions have been investigated during this SBIR Phase I program. As a result, several new acousto-optic tunable filters have been built and tested. The program is highlighted by

1) Design, fabrication and experimental demonstration of a novel TeO_2 near-collinear acousto-optic tunable filter has been designed, fabricated and tested. *The device exhibits a 1.29 nm spectral resolution and a 160 mw RF drive power at 1523 nm.*

2) Design, fabrication and experimental demonstration of a novel polarization insensitive TeO_2 near-collinear acousto-optic tunable filter. For random input light, *an overall insertion loss < 3 dB* has been achieved.

3) Design, fabrication and experimental demonstration of a novel collinear acousto-optic tunable filter. The filter exhibits a *spectral resolution of 1.12 nm @ 1523nm* with a low insertion loss.

4) The commercial spin-off also has been accomplished at the end of the program. A commercially available fiber pigtailed near-collinear AOTF is shown in the photo. Commercial sales have been generated and new AOTFs have been delivered to customers for applications in optical fiber communications and sensors.

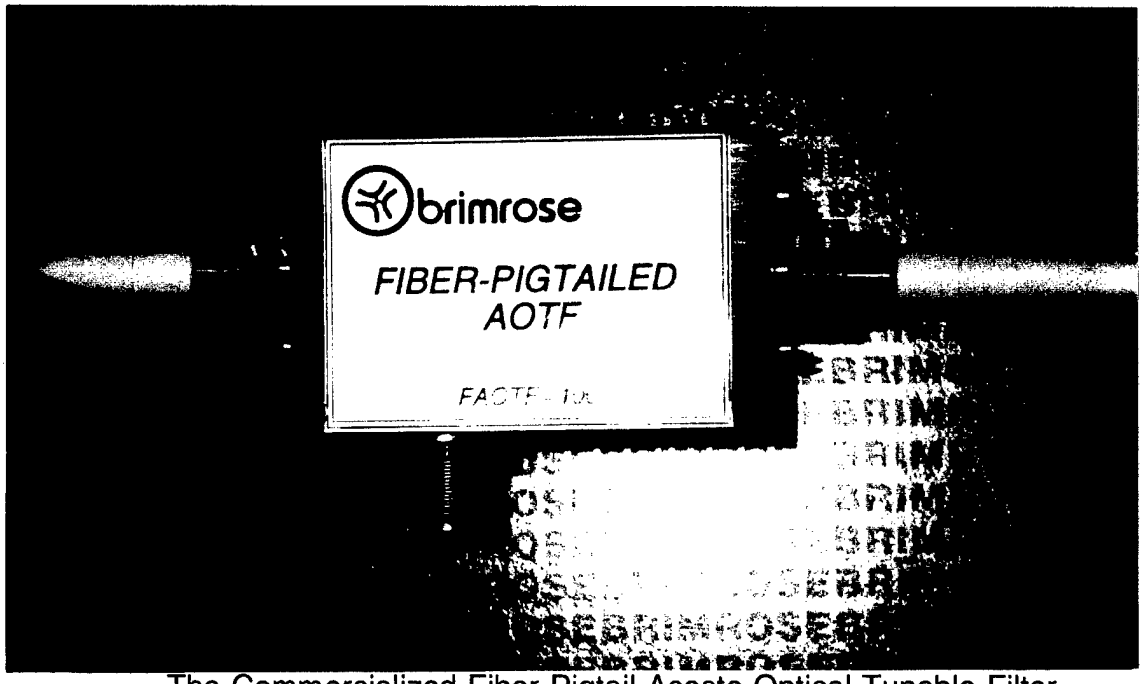

The Commercialized Fiber Pigtail Acosto-Optical Tunable Filter

II. List of Figures

Figure 14. Spectral response of the collinear AOTF @ 1523 nm.

Figure 15. Diffraction efficiency vs. drive power of the new collinear AOTF.

III. List of Tables

1.0 OBJECTIVES

The objective of this SBIR Phase I program is to develop a compact tunable optical filter for wavelength division demultiplexing in local area networks.

2.0 BACKGROUND

There is an increased interest in the use of wavelength division multiplexing to increase the bandwidth and connectivity in advanced military local area networks. This interest has resulted in a need for compact wavelength division demultiplexers which are compatible to the size and power requirements of a typical fiber optical system.

2.1 Acousto-Optic Tunable Filters (AOTFs)

An AOTF is based on the acoustic diffraction of light in an anisotropic medium and consists of a piezoelectric transducer bonded to a birefringent crystal. When the transducer is excited by an applied RF signal, acoustic waves are generated in the medium. The propagating acoustic waves produce a periodic modulation of the index of refraction. This provides a moving phase grating which, under appropriate conditions, will diffract portions of an incident light beam. For a fixed acoustic frequency, only a limited band of optical frequencies can satisfy the phase-matching condition and be cumulatively diffracted. As the RF frequency is changed, the center optical passband is changed accordingly so that the phase matching condition is maintained.

Anisotropic acousto-optic diffraction involves a 90 degree rotation of the polarization plane of the diffracted wave. If an AOTF is sandwiched between crossed polarizers, only those spectral wavelengths within the AOTF passband are polarization converted (see Figure 1). Wavelengths outside the passband are not rotated and are therefore blocked.

Bulk AOTF devices are now commercially available. They are usually based on a non-collinear configuration in which the acoustic wave and optic wave are almost perpendicular to each other (see Figure 2). For example, Brimrose currently produces two series of bulk AOTF devices which cover the wavelength region 0.2-5.5μm with a resolution of 0.1-10nm. The major drawback of bulk AOTF devices is the required RF drive power, which is typically 1-3 Watts in the infra-red region. The advantages are easy fabrication and low optical insertion loss.

2.2 Integrated-Optic Acousto-Optic Tunable Filter (IOAOTF)

The same kind of acousto-optic interaction also occurs in thin film waveguides when both optical and acoustic fields are confined within a very thin (several micrometers) surface guiding layer. An integrated-optic AOTF, with typical dimensions of 10x5x1mm, is illustrated in Figure 3. The incident light is first prepared in a single propagating mode, such as the TE mode. A periodic perturbation is then applied which causes the original mode to transform to the orthogonal mode, the TM mode. In this case, the perturbation

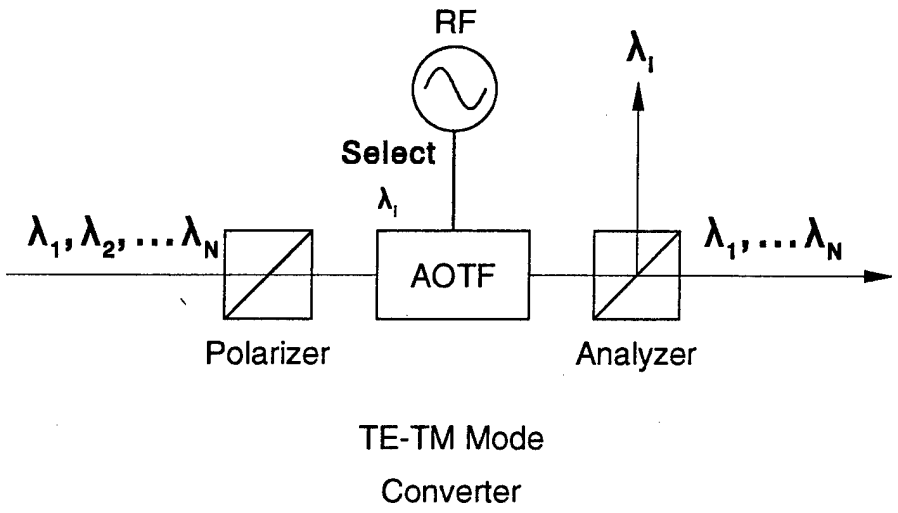

Figure 1 Schematic drawing of an AOTF. It acts like a TE-TM mode converter sandwiched between a pair of crossed polarizers. The wavelength tuning can be accomplished by changing the RF frequency.

is created by surface acoustic waves (SAWs) which propagate collinearly with the optical waves. The SAWs are generated by a thin film metal inter-digital transducer (IDT) deposited onto the surface of the substrate. Acoustic waveguides allow reduced RF drive power requirements by laterally confining the SAW beam. The periodic modulation of the material's refractive index permits only a narrow spectral region, of wavelengths which satisfy the mode coupling conditions, to be orthogonally rotated. Separation of the two orthogonally polarized modes result in a highly selective wavelength filter. This separation can be achieved by an integrated polarizer or an external polarizing beam splitter.

In comparison to the bulk AOTF, the IOAOTF can achieve very high diffraction efficiency with a much lower acoustic drive power. This is due to the fact that the diffraction limitations of interaction length (L) can be eliminated by channel waveguides for both the optical and acoustic beams. IOAOTFs can therefore achieve high diffraction efficiency (typically >98%) with substantially less RF power than their bulk-optic counterparts. This, coupled with their compatibility with optical fibers make IOAOTFs extremely attractive for applications in fiber based systems. The main drawback of an IAOTF is its high insertion loss due to the mode mismatch between fiber and Ti-$LiNbO_3$ waveguide.

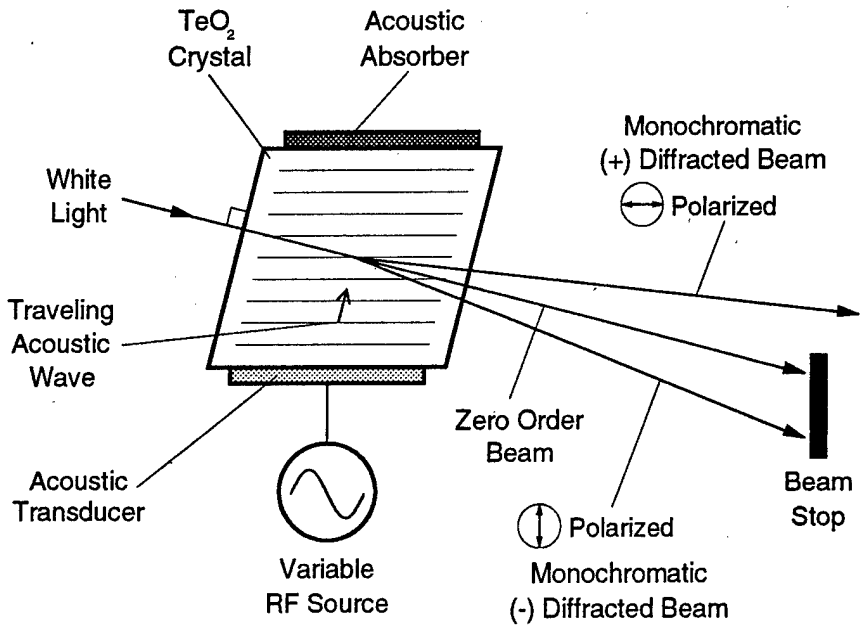

Figure 2. Schematic representation of a TeO_2 non-collinear AOTF.

2.3 The State of Art Limitations of Acousto-Optic Filters

Table I is a list of the performance of the required filter and the typical performance of two types of acousto-optic filters. As shown in the table, neither the bulk non-collinear AOTF nor the integrated AOTF can satisfy all the required specifications.

1) **Transmission Requirement**: In order to satisfy the 50% transmission, the filter must be constructed in a way that is insensitive to the polarization of the incoming light.

2) **Resolution Requirement**: For the bulk non-linear AOTF, the spectral resolution can not be increased to better than 2 nm, due to the limited acousto-optic interaction length.

3) **Insertion Loss:** For the IOAOTF, the 4-5 dB insertion loss is very difficult to further reduce due to the mode mismatch.

So there are needs of innovative approaches in which all the requirements of the desired filter can be satisfied.

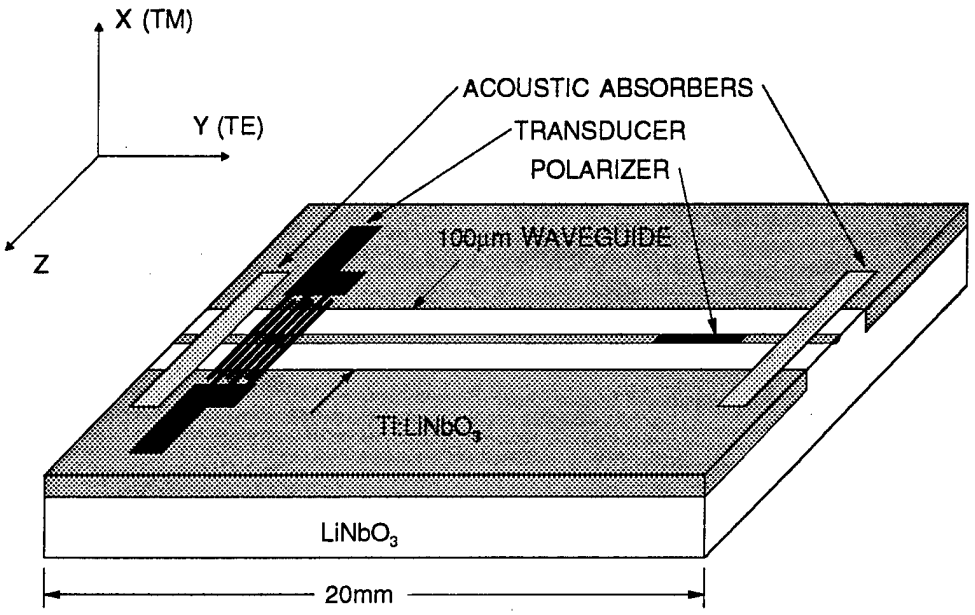

Figure 3. Schematic of an integrated-optic acousto-optic tunable filter (IOAOTF) in a Ti:$LiNbO_3$ waveguide.

Table I: Comparison of the performance of listed filters

	Required Filter	Non-Collinear AOTF	Integrated AOTF
Spectral Range	0.8-1.6 μm	0.8-1.6 μm	0.8-1.6 μm
Resolution	1 nm	**4-6 nm @ 1550 nm**	1-2nm @ 1550nm
Bandwidth	120 nm	800 nm	200 nm
Accuracy	1 nm	< 1 nm	< 1nm
Transmission	> 50%	**40-49%** (80-98%) [(a)]	**45-49%**(90-98%)[(a)]
Extinction Ratio	-30 dB	< -30 dB	< -30 dB
Insertion Loss	3 dB	< 1 dB	**4-5 dB**
Power	? (20 Volt)	1-2 Watt	100-200 mW
Physical Size	1"x1"x0.125"	<1"x0.5"x0.5"	<1.5"x0.5"x0.1"

(a) For polarization insensitive devices.

3.0 TECHNICAL APPROACH: Near-Collinear/Collinear AOTF

Novel concepts of near-collinear/collinear acousto-optic interaction have been investigated during this Phase I program.

A traditional non-collinear AOTF based on bulk TeO_2 are advantageous due to their high figure of merit, easy fabrication and negligible coupling loss. Unfortunately, an enormous energy walk-off of an anisotropic acoustic beam and a non-critical phase matching (NPM) configuration (Figure. 2) results in the shortening of the interaction length (L) down to less than 3/4 of the transducer length. The interaction length is the crucial parameter which both resolution ($\delta\lambda \propto 1/L$) and drive power ($P_a \propto 1/L^2$) depend on. The short interaction length results P_a=1-2 Watts and $\delta\lambda$=4-6 nm at 1.55 μm for a conventional TeO_2 AOTF.

The near-collinear (or collinear) configuration with the longest possible interaction length, outlined by the dashed-dotted line in Figure 4 can drastically improve both the efficiency and the spectral resolution of the AOTF:

$$\delta\lambda = \frac{0.9\lambda^2}{L\,\Delta n\,\sin\theta_e^2} \qquad \textbf{(1)}$$

where λ is the wavelength and Δn is the birefringence. From Eq.(1), L = 20 mm is required to obtain $\delta\lambda$ =1 nm FWHM with θ_e = 60°, at 1.55 μm.

In this new configuration the requirement of the NPM has been relaxed, and the first order angular wavelength tunability:

$$\frac{d\lambda}{d\theta_e} = \lambda[2\,\cot\theta_e - \tan(\theta_a - \theta_e)] \qquad \textbf{(2)}$$

is not zeroed any more and reaches a value of 0.42 nm/mrad (in the air) with θ_a = 88°. This means that the thorough collimation of the optical beam is required to avoid the divergence-induced spectral blurring. Fortunately, in fiber optic communication, it is relatively easy to get a beam well collimated by using a fiber pigtailed collimator. If the collimated beam with 1 mm FWHM has 0.69 mrad FWHM diffraction divergence, which would cause less than 5% broadening of the theoretically estimated $\delta\lambda$ = 1 nm.

The first order polar angular phase mismatch is not vanishing either, unlike it was at the NPM, and the new AOTF will have the polar acceptance angle:

$$\delta\theta_e = \frac{0.9}{L\,\Delta n\,\sin^2\theta_e\,[2\,\cot\theta_e - \tan(\theta_a - \theta_e)]} = 2.4\ mrad\ \ (\ in\ the\ air\ ) \qquad (3)$$

which is still large enough to accept the collimated beam as mentioned above, without any vignetting.

The azimuthal acceptance is not influenced by the breach of the NPM condition and remains of the same quadratic type and, hence, is just as wide as it was for the conventional AOTF.

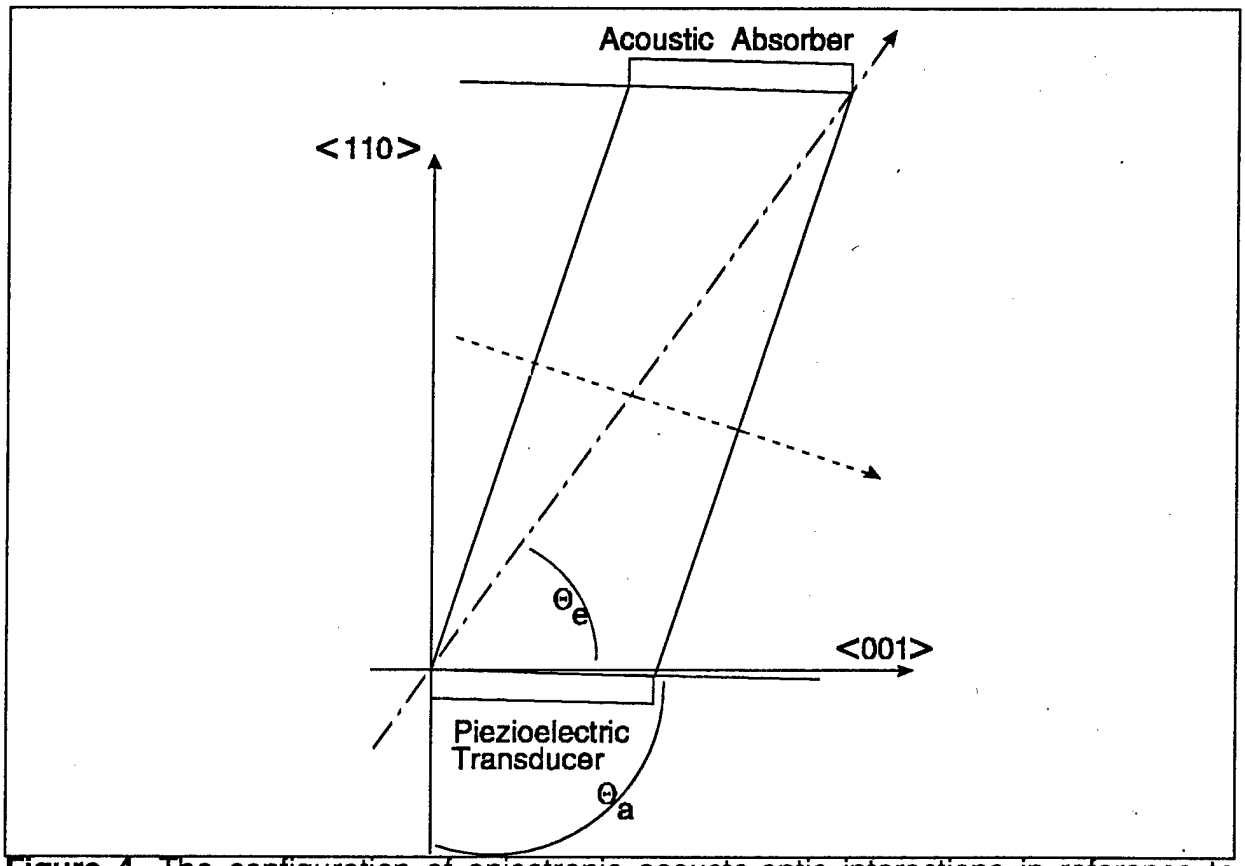

Figure 4. The configuration of anisotropic acousto-optic interactions in reference to crystallographic axes of TeO_2. Dashed line represents the light propagation direction in a conventional device; dashed-dotted line represents the light propagation direction in the new near-collinear device. θ_a and θ_e are the polar angles for the acoustic shear and extraordinary optic wavevector. respectively.

Another advantage gained by this new AOTF, due to the proximity to the collinearity, is the significant reduction of the angular deflection of the filtered optical beam, which in turn allows coverage of a broad wavelength range with the same low fiber coupling loss.

4.0 DEVICE FABRICATION

The AOTF manufacturing flow chart is illustrated in Figure 5.

4.1 Optical Substrate Preparation

The bulk TeO_2 crystal was x-ray oriented using a Laue back reflection technique. The crystal boule was cut with the proper orientation for the AOTF. The orientation included repeated Laue, grinding, blocking, and milling of TeO_2 to achieve acceptable angle alignment of the [110] axes. A detailed procedure along with the final Laue exposures were recorded. After orientation, the crystal was blocked to saw on the desired axis to produce a slab that yields a strip for fabrication. In the next step of the fabrication process, the cut sample was then prepared with the bonding and optical surface.

4.2 Shear Mode Transducer

The shear mode $LiNbO_3$ transducer was also concurrently being produced for bonding to the AOTF optical substrates. These pieces were prepared in slab form. A slab 1/4"x2" was cut from an existing oriented boule and the bonding faces were polished as one unit. The particle motion was aligned appropriately in the proper direction.

4.3 Bonding Process

After deblocking, the substrate strips were bonded with a shear mode transducer. Thinning of the shear mode devices ended with the frequency of 30-150 MHz as the desired acousto-optic objective. The final thickness of the transducers was calculated based upon the following formula: $d=V/2f$, where d, V and f are the thickness, acoustic velocity and desired frequency. Since the acoustic frequency in the shear mode $LiNbO_3$ is 4800m/s, the needed transducer thickness for 100 MHz operations is 24 μm. During the thinning process, the transducers were closely monitored with a Taylor-Hobson Tally Surf. Resolution of the instrument is 400 Angstroms. After the optical substrate strip was lapped down to a frequency of 30-100 MHz, the strip was sawed into devices to expose the optical faces. The optical faces were ground and polished.

4.4 Electrical Impedance Matching/Optical Testing

In the next step, the device is mounted to a mechanical supporting base and the top electrode is wired bonded to a microwave strip line. The impedance matching is performed by using an on-line microwave network analyzer which displays Smith charter as well as the standing wave ratio (SWR) over the whole frequency band. A 3dB 50Ω impedance matching is achieved between 30-100 MHz which is corresponding to the InGaAs detector spectral response curve 1.0-2.5 μm.

Finally, the optical parameters are tested. The efficiency and resolution is measured by

using lasers at different wavelengths. By sweeping the frequency of a RF source around a specific laser wavelength (with infinitesimal linewidth), the peak optical transmission as well as the bandpass is measured.

The performance of the fabricated device agrees well with the designed parameters and thus is satisfactory for system applications.

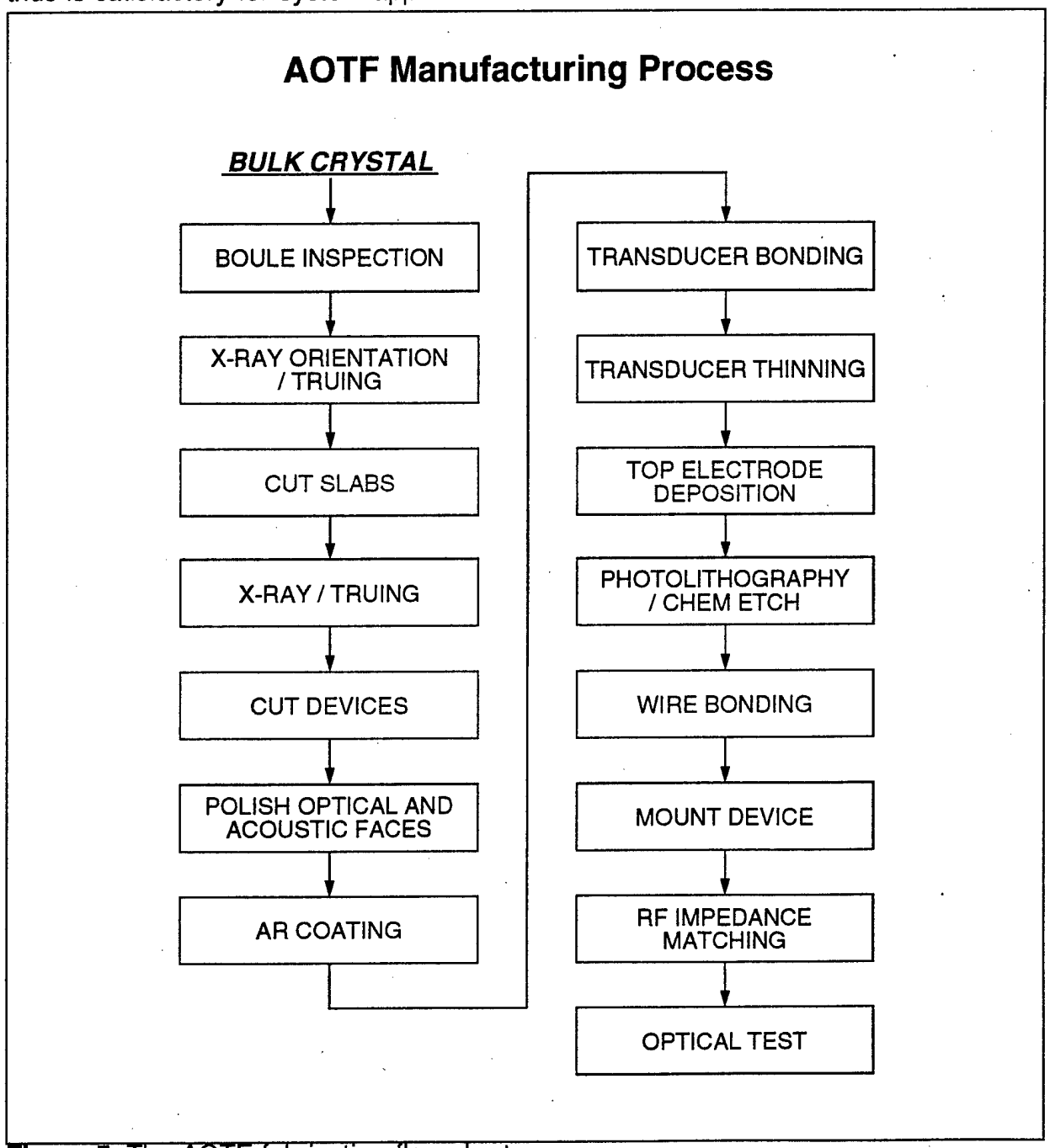

Figure 5. The AOTF fabrication flow chart.

5.0 EXPERIMENTAL RESULTS

5.1 Near-Collinear Acousto-Optical Tunable Filter

The conceived new near-collinear AOTF was designed with the above mentioned design parameters and realized using a 6 mm × 12 mm × 25 mm (0.24"x0.48"x1") TeO_2 crystal with a 3 mm × 6 mm shear mode piezoelectric $LiNbO_3$ transducer. Figure 6 is a schematic illustration of the near-collinear AOTF. Figure 7 is a photo which shows a fiber pigtailed near-collinear AOTF. The light input is launched into the AOTF from the single mode fiber in the left and diffracted light is coupled into an optical fiber in the right. The wavelength tuning is controlled through a RF input (a SMA connector at the top). The impedance matching circuit is shown at the bottom of the device.

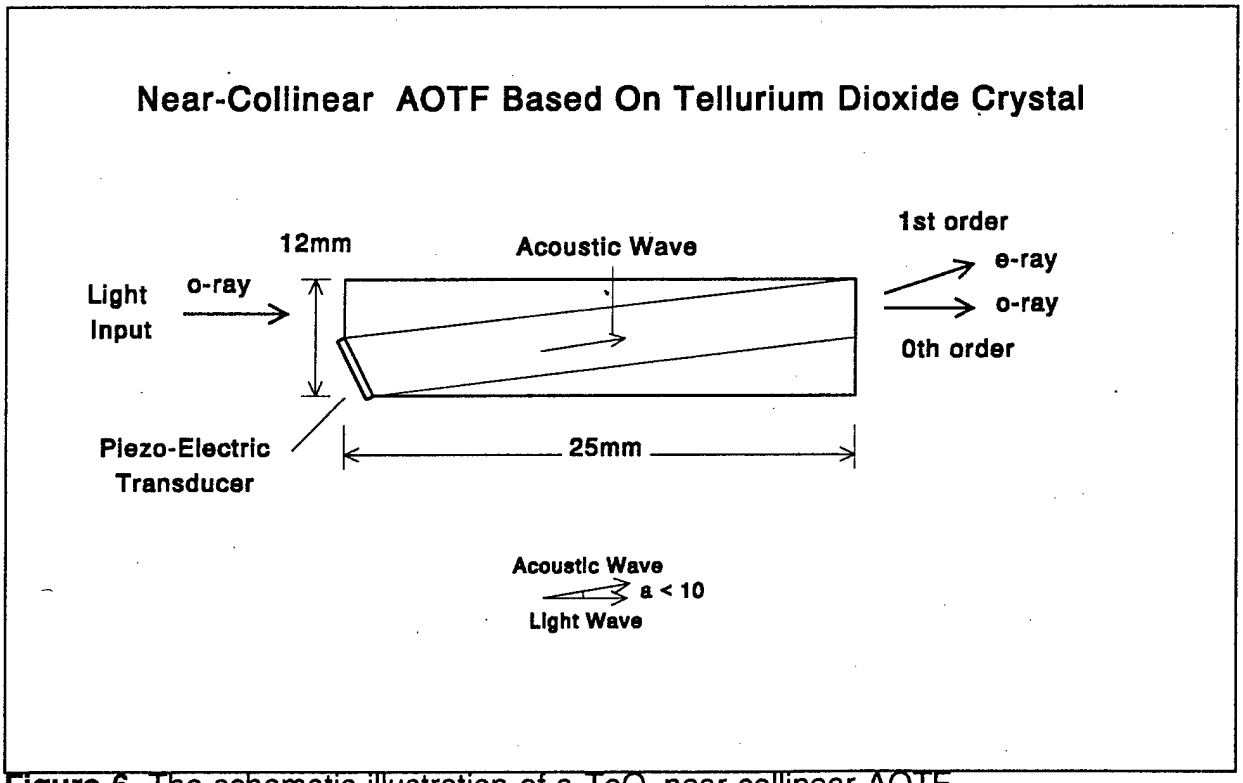

Figure 6. The schematic illustration of a TeO_2 near-collinear AOTF.

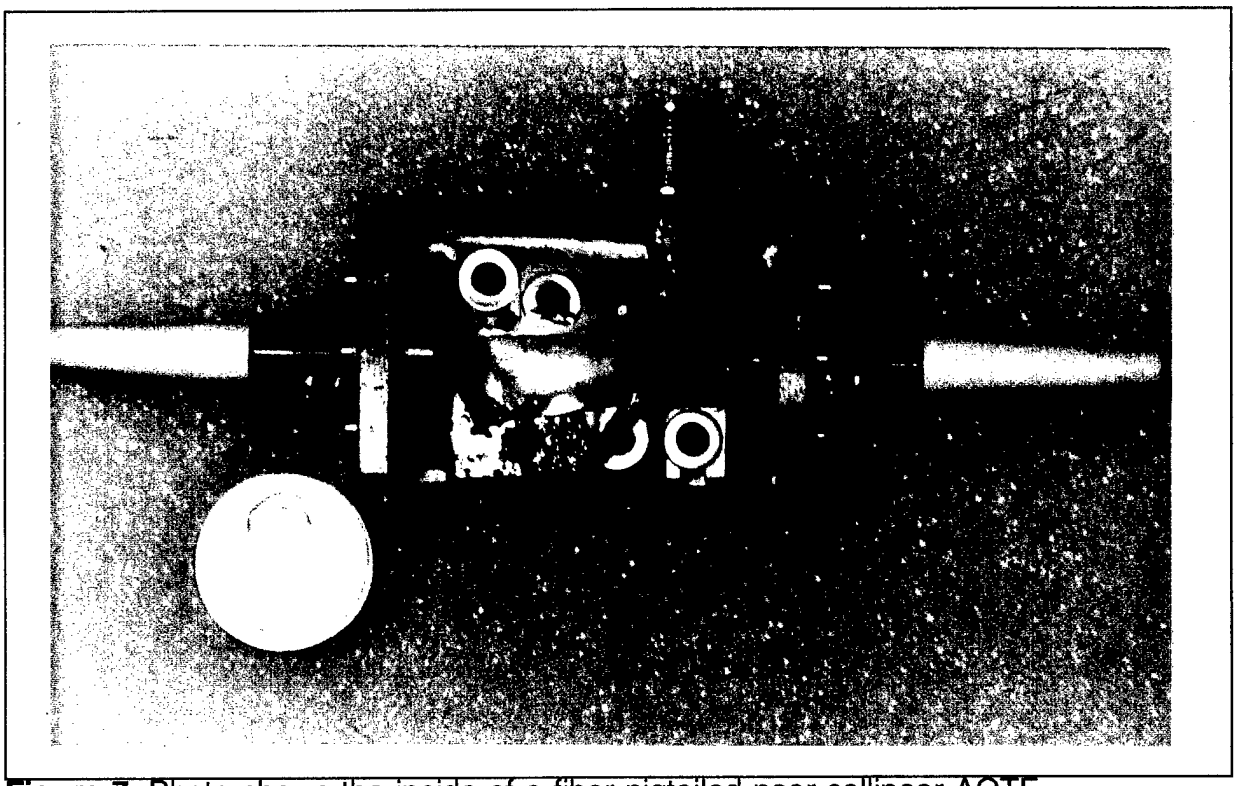

Figure 7. Photo shows the inside of a fiber pigtailed near-collinear AOTF.

The measurements have confirmed all the new expected features. Figure 8 shows the plotted frequency response of the new AOTF for 1523 mn He-Ne laser. The center frequency of 48.73 MHz agrees with the tuning relation:

$$\lambda = \frac{\Delta n \; V_a}{f} \frac{\sin^2\theta_e}{\cos(\theta_a - \theta_e)} \qquad \textbf{(4)}$$

and the FWHM of the frequency response δf = 41.2 kHz corresponds to the spectral resolution $\delta\lambda$ = 1.29 μm, slightly broader than expected, which is explainable by the excessive divergence of a narrow (< 0.5 mm) He-Ne laser beam.

Figure 9 represents the dependence of the diffraction efficiency vs the drive power. It shows that a high conversion efficiency (> 50%) was reached at a relatively low RF power level (< 160 mW). Due to the low coupling losses between the device and fibers, the overall throughput per RF power is comparable to commercially available integrated AOTFs. Further increasing of the efficiency with lower RF power can be achieved with further reduction in the size of the acoustic transducer.

5.2 Polarization Insensitive Near-Collinear Acousto-Optical Tunable Filter

As indicated by the previous discussions, there is a 3 dB loss in a regular AOTF for randomly polarized light. In order to eliminate this 3 dB loss, a polarization insensitive near-collinear AOTF has been fabricated and tested. Figure 10 is a schematic illustration of the operation principle of the device. Two additional polarization separation/combination stages are added to a regular AOTF. Figure 11 shows a working polarization insensitive AOTF. In the photo, the input is launched from the right and exits from the left. The polarization beam splitter/combiner and half wave plate are boned into an integrated block and attached to the AOTF directly. The top of the device shows microwave strip-line circuit of the impedance matching network.

Table II: The Performance Comparison of The Polarization Sensitive/Insensitive Near-Collinear AOTF and The Required Filter.

	Required Filter	Near-Collinear AOTF	Polarization Insensitive Near-Collinear AOTF
Spectral Range	0.8-1.6 μm	0.8-1.6 μm	0.8-1.6 μm
Resolution	1 nm	1.29 nm @ 1532 nm	1.29 nm @ 1532 nm
Bandwidth	120 nm	300 nm	300 nm
Accuracy	1 nm	<1 nm	< 1 nm
Transmission	> 50%	60 % [a]	60 %
Extinction Ratio	-30 dB	<-30 dB	< -30 dB
Insertion Loss	3 dB	< 0.5 dB **(+ 3 dB)**[b]	< 0.5 dB
Power	? (20 Volt)	150 mW	150 mW
Physical Size	1"x1"x0.125"	<1"x0.5"x0.5"	<1.5"x0.5"x0.5"

(a) For polarized incoming light.
(b) The loss due to random polarized incoming light.

Table II is a performance comparison of the polarization sensitive/insensitive near-collinear device and the required filter. The overall performance is improved dramatically in comparison to their conventional counterparts as shown in Table I.

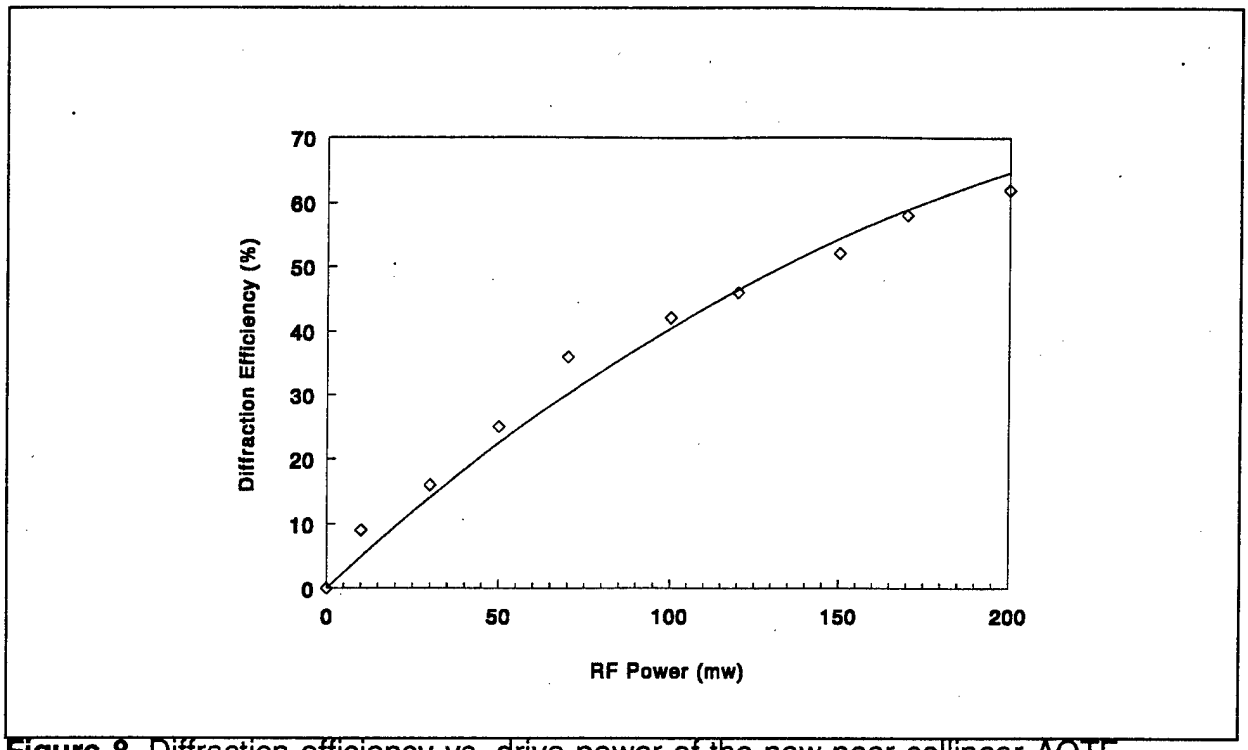

Figure 8. Diffraction efficiency vs. drive power of the new near-collinear AOTF.

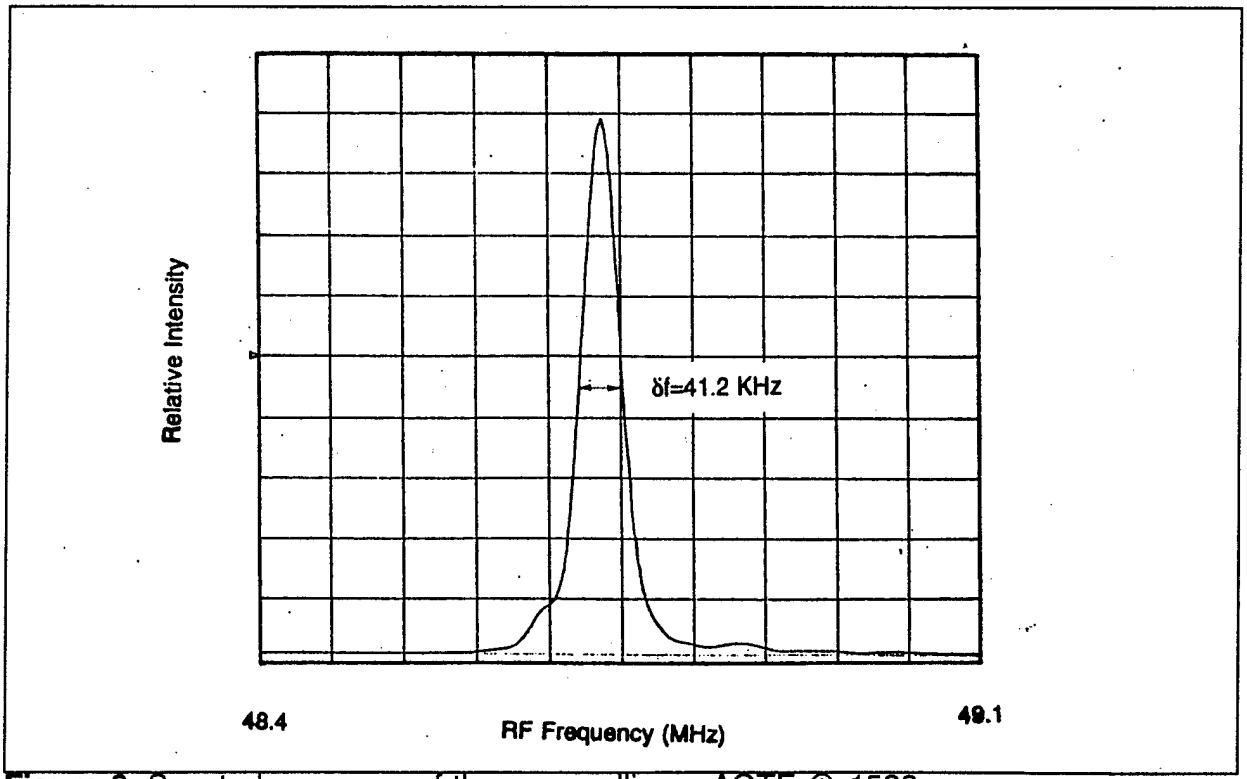

Figure 9. Spectral response of the near-collinear AOTF @ 1523 nm.

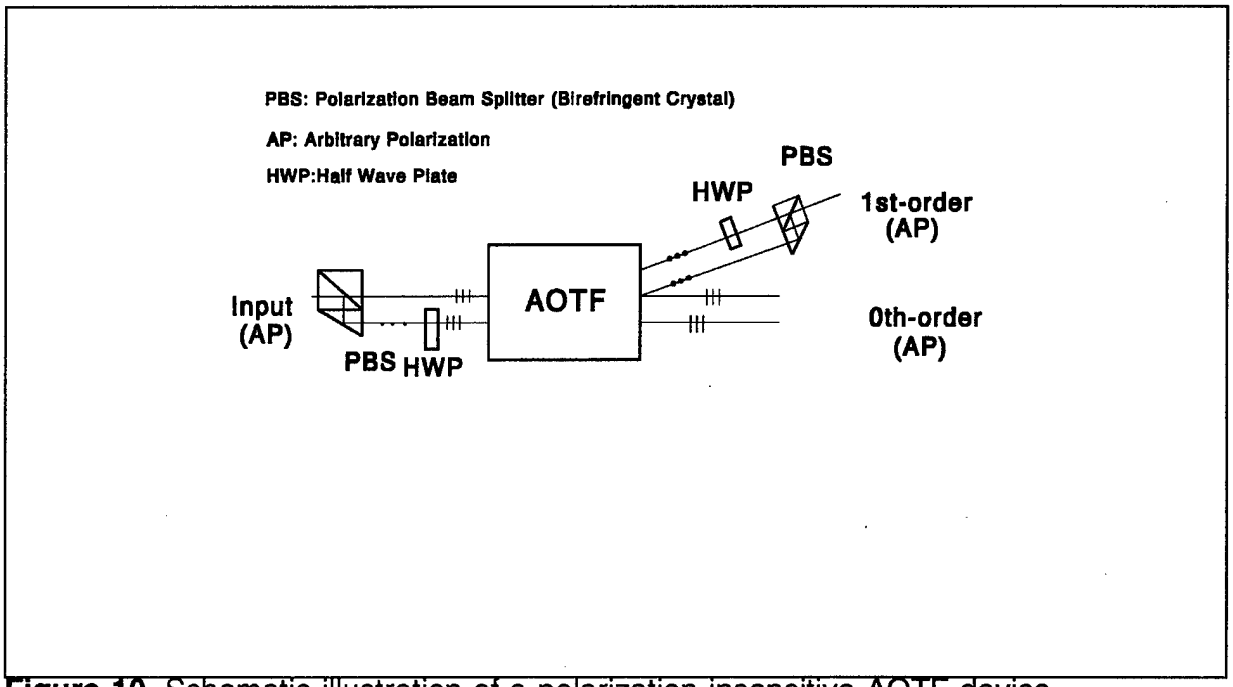

Figure 10. Schematic illustration of a polarization insensitive AOTF device.

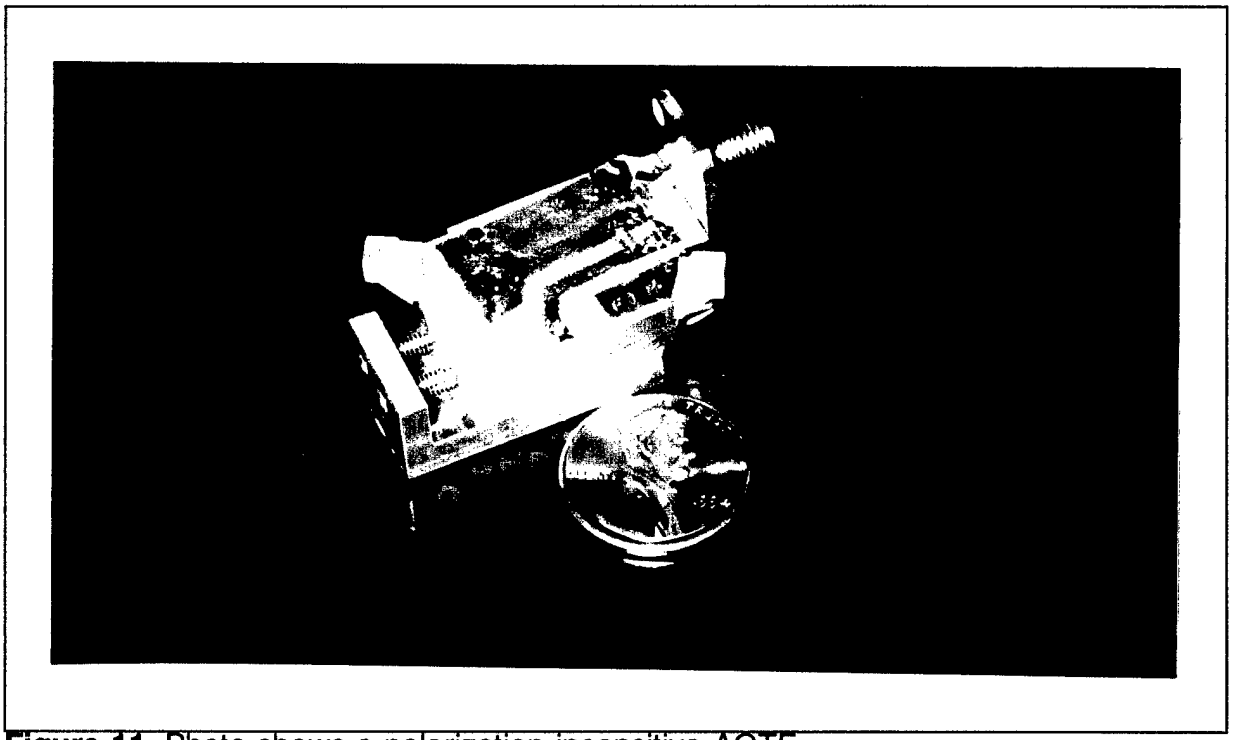

Figure 11. Photo shows a polarization insensitive AOTF.

5.3 Collinear Acousto-Optical Tunable Filter

Also investigated in this Phase I program is a collinear AOTF. Figure 12 is the schematic illustration of the device. An ordinary polarization is chosen for the incident optical beam. The acoustic wave launched from the transducer is reflected from the prism surface which is chosen so that the acoustic group velocity is collinear with the incident ordinary ray. When the momentum matching condition is satisfied, an extraordinary polarized diffracted optical beam at the passband wavelength will generated in the crystal. The diffracted narrowband optical beams coupled out of the prism surface may be selected using polarizers or spatial separations.

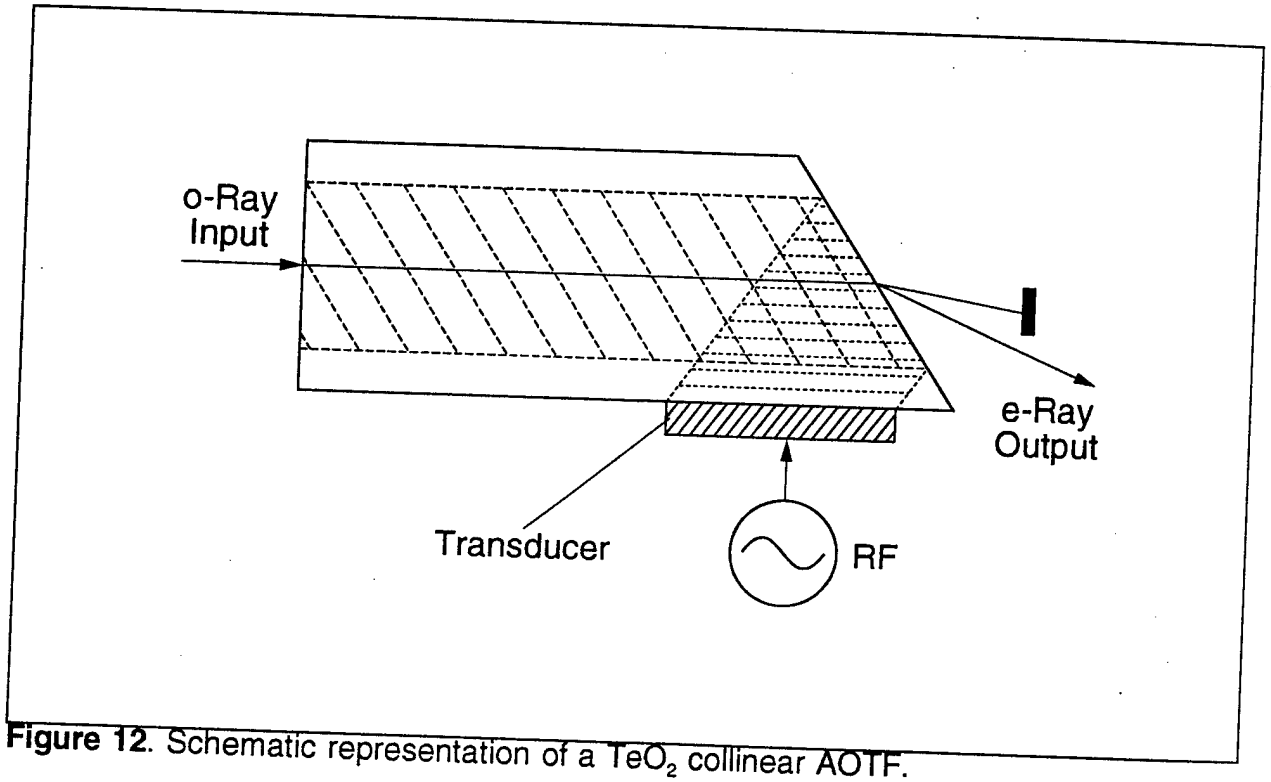

Figure 12. Schematic representation of a TeO_2 collinear AOTF.

Figure 13 is a photo showing a fabricated TeO_2 collinear AOTF. The crystal is measured at 6x6x25 mm. In operation the input light is coupled into the device from the bottom of the picture and coupled out from the top. Also shown in the picture is a RF coaxial cable and strip-line structure attached to the AOTF.

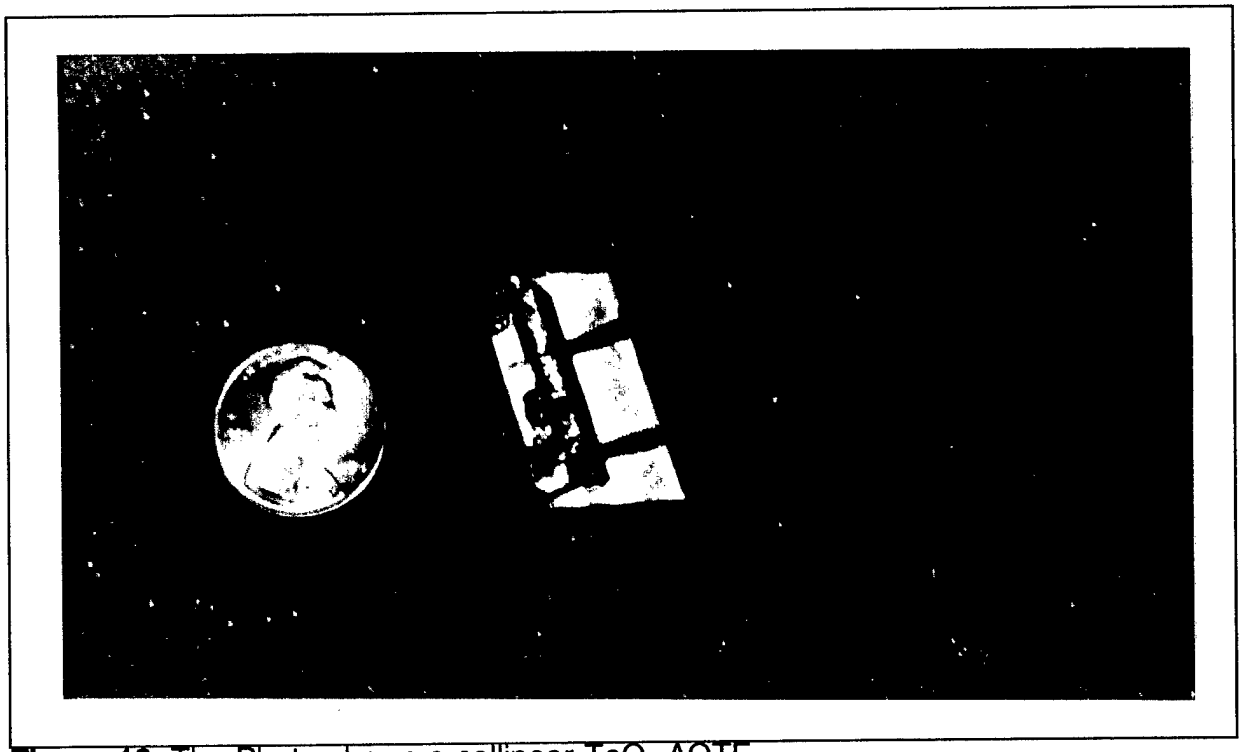

Figure 13. The Photo shows a collinear TeO_2 AOTF.

Figure 14 shows spectral response of the collinear AOTF at 1.523 μm. Figure 15 shows diffraction efficiency vs. drive power of the new collinear AOTF.

As noticed, the required RF power is much larger than the estimated value. It may be due to the combined contributions from a poor bonding quality and the acoustic walk-off due to inaccurate crystal cutting angle. Much better results should be expected in the future.

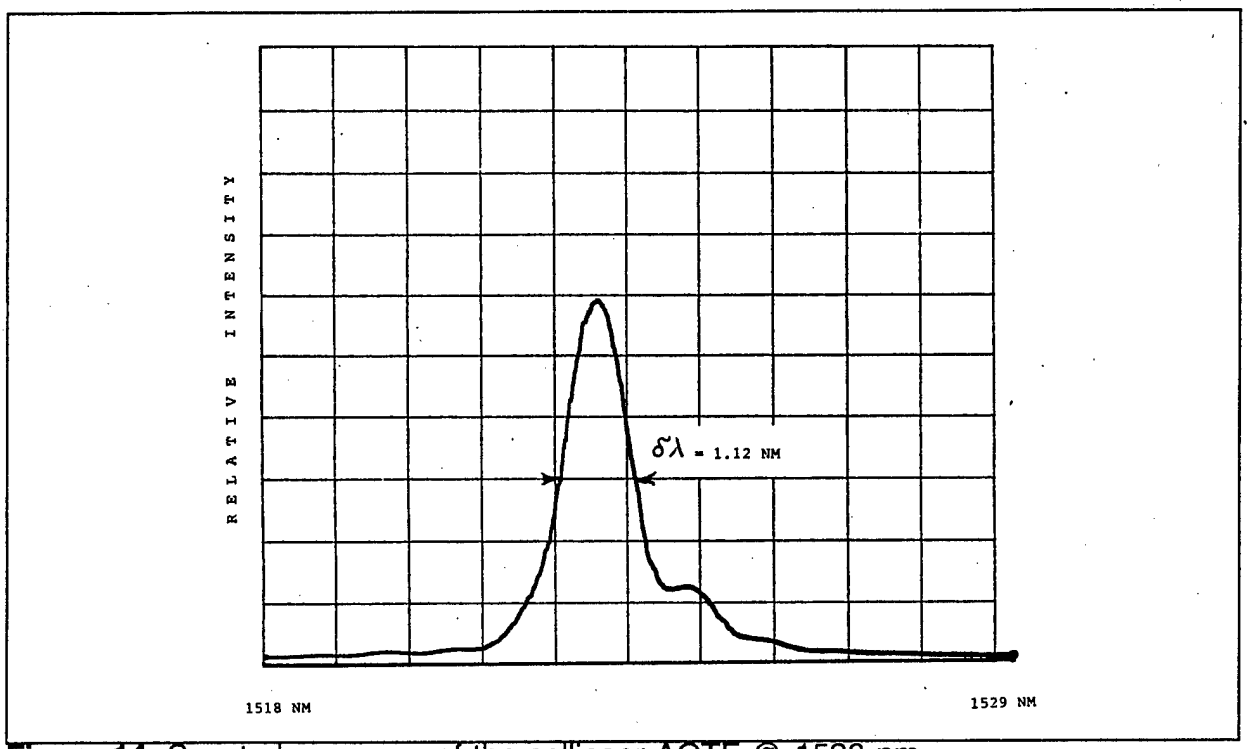

Figure 14. Spectral response of the collinear AOTF @ 1523 nm.

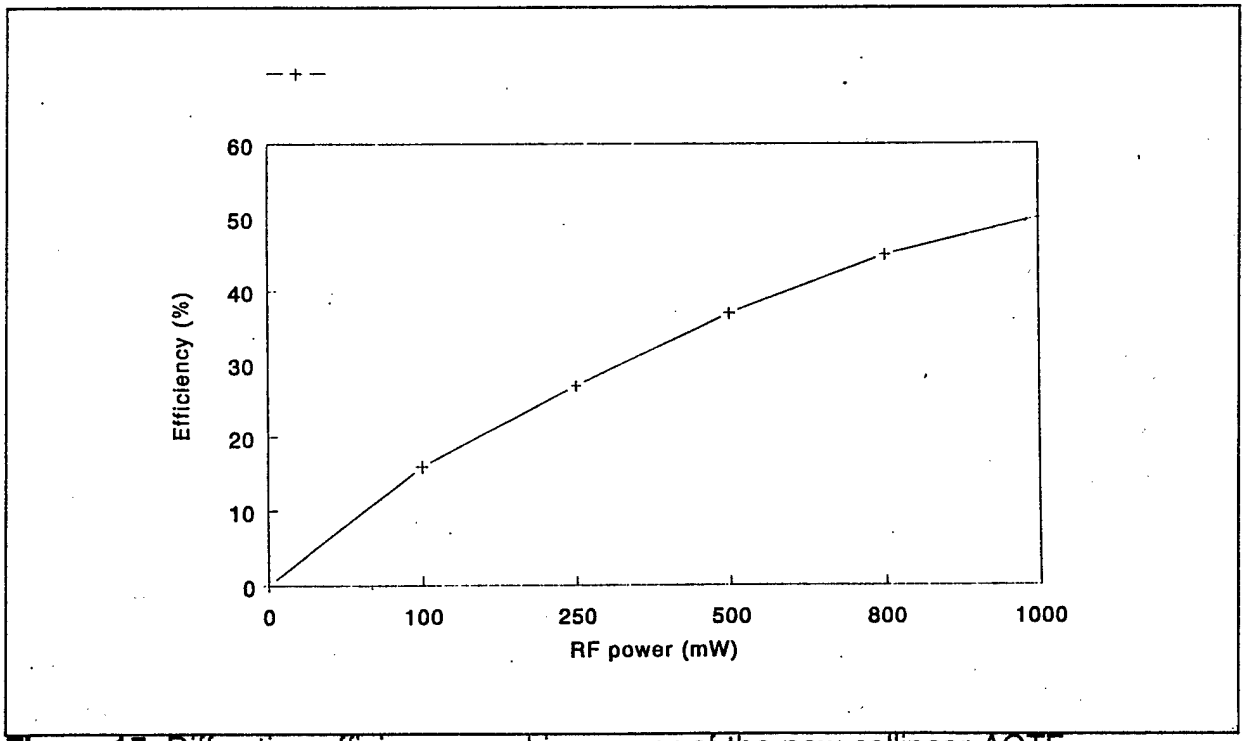

Figure 15. Diffraction efficiency vs. drive power of the new collinear AOTF.

6.0 CONCLUSIONS AND PHASE II PROGRAM

In conclusion, novel concepts of near-collinear/collinear acousto-optic interactions have been investigated during this SBIR Phase I program. As a result, several new acousto-optic tunable filters have been built and tested. The program is highlighted by

1) Design, fabrication and experimental demonstration of a novel TeO_2 near-collinear acousto-optic tunable filter has been designed, fabricated and tested. *The device exhibits a 1.29 nm spectral resolution and a 160 mw RF drive power at 1523 nm.*

2) Design, fabrication and experimental demonstration of a novel polarization insensitive TeO_2 near-collinear acousto-optic tunable filter. For random input light, *an overall insertion loss < 3 dB* has been achieved.

3) Design, fabrication and experimental demonstration of a novel collinear acousto-optic tunable filter. The filter exhibits a *spectral resolution of 1.12 nm @ 1523nm* with a low insertion loss.

4) The commercial spin-off also has been accomplished at the end of the program. A commercially available fiber pigtailed near-collinear AOTF is shown in the photo. Commercial sales have been generated and new AOTFs have been delivered to customers for applications in optical fiber communications and sensors.

In the Phase II program, several new AOTFs will be demonstrated and commercialized with improvements in the areas of

a) operating power level,
b) insertion loss,
c) efficiency,
d) spectral,
e) RF control module.

7.0 REFERENCES

1. X. Wang, Laser Focus World, Vol 28, No. 5, PP. 173-180, (1992).

2. X. Wang, Opto News & Letters, Vol. 37, No. 37-38, (1992).

3. I. C. Chang, Appl. Phys. Lett. 25, 370 (1974).

4. X. Wang, D. E. Vaughan and V. Pelekhaty, Rev. Sci. Instrum. 65(12) (1994).

5. X. Wang, H. Y. Zhang, J. Soos and J. Crisp, Pittcon'94, Paper 1245, Chicago, Il, Fab. 27 - Mar. 4 (1994).

6. X. Wang, J. Soos, Q. Li and J. Crystal, Process Control and Quality, **5**, 9 (1993).

7. X. Wang, H. Y. Zhang, J. Soos and J. Crisp, East Analytical Symposium, Paper 26, Somerset, NJ, Nov. 15 (1993).

8. E. N. Lewis, P. J. Treado and J. W. Levin, Appl. Spectrosc. 47, 539 (1993).

9. P. J. Treado, E. N. Lewis and J. W. Levin, Appl. Spectrosc. 46, 1211 (1992).

10. Y. Ohmachi and J. Noda, IEEE J. Quantum Electron., **QE-13**, 43 (1977).

11. L.N. Binh and J. Livingstone, IEEE J. Quantum Electron., **QE-16**, 964 (1980).

12. K. W. Cheung, IEEE J. Select. Areas in Comm., **8**, 1015, (1992).

13. *Properties of Lithium Niobate*. emis data review series No.5. IEE Inspec,, (1989).

14. Arnold Eilert and David Wetzel, Private Communication (1992).

15. D.A. Smith and J.J. Johnson, Appl. Phys. Lett. **61**, 1025 (1992).

16. A. Kar-Ray and C.S. Tsai, Integrated Photonics Research, **ME2-1**, 90 (1992).

17. D. A. Smith, J. E. Baran and K. W. Cheung, Appl. Phys. Lett., **56**, 209 (1990).

18. T. Pohlmann, A. Neyer and E. Vogues, IEEE J. Quantum. Electron., **27**, 602 (1991).